



Citation for published version:

Weber, M, Mackenzie, AB, Bull, SD & James, TD 2018, 'Fluorescence based Tool to Detect Endogenous Peroxynitrite in M1-Polarized Murine J774.2 Macrophages', *Analytical Chemistry*, vol. 90, no. 17, pp. 10621–10627. <https://doi.org/10.1021/acs.analchem.8b03035>

DOI:

[10.1021/acs.analchem.8b03035](https://doi.org/10.1021/acs.analchem.8b03035)

Publication date:

2018

Document Version

Peer reviewed version

[Link to publication](#)

This document is the Accepted Manuscript version of a Published Work that appeared in final form in *Analytical Chemistry*, copyright (C) American Chemical Society after peer review and technical editing by the publisher. To access the final edited and published work see: <http://dx.doi.org/10.1021/acs.analchem.8b03035>

University of Bath

General rights

Copyright and moral rights for the publications made accessible in the public portal are retained by the authors and/or other copyright owners and it is a condition of accessing publications that users recognise and abide by the legal requirements associated with these rights.

Take down policy

If you believe that this document breaches copyright please contact us providing details, and we will remove access to the work immediately and investigate your claim.

Fluorescence based Tool to Detect Endogenous Peroxynitrite in M1-Polarized Murine J774.2 Macrophages

Maria Weber^{†,‡}, Amanda B. Mackenzie^{*·ll·§}, Steven D. Bull[‡], Tony D. James^{*·‡·λ}

[†] Centre for Doctoral Training, Centre for Sustainable Chemical Technologies, University of Bath, Bath BA2 7AY, UK

[‡] Department of Chemistry, University of Bath, Bath BA2 7AY, UK

^{ll} Department of Pharmacy and Pharmacology, University of Bath, Bath BA2 7AY, UK

[§] Centre for Therapeutic Innovation, University of Bath, Bath BA2 7AY, UK

^λ Department of Materials and Life Sciences, Faculty of Science and Technology, Sophia University, 7-1 Kioi-cho, Chiyodaku, Tokyo 102-8554 Japan

* E-mail: A.Mackenzie@bath.ac.uk .T.D.James@bath.ac.uk

ABSTRACT: Oxidative stress and inflammation are intrinsically linked to each other in addition they are implicated in the evolution and progression of non-communicable diseases (NCD). Large amounts of reactive oxygen species (ROS) are generated as part of the immune response towards NCD. Among all the ROS species, peroxynitrite (ONOO⁻) has the shortest half-life with < 20 ms under typical physiological conditions. Hence, detecting ONOO⁻ and studying its generation *in vitro* allows for a better understanding of inflammatory processes. We demonstrate that peroxyresorufin-1 (PR1) is a selective and sensitive ONOO⁻ fluorescence based sensor in J774.2 macrophages. PR1 was able to detect changes in ONOO⁻ production upon investigation of different factors: enhanced generation of ONOO⁻ through LPS and IFN- γ as well as diminished ONOO⁻ production with the introduction of superoxide scavengers and nitric oxide synthase inhibitors. Our study validates PR1 as an effective tool for the detection of ONOO⁻ in J774.2 murine macrophages and should allow for further elucidation of ROS biology and chemistry.

In recent years, growing evidence has linked non-communicable diseases (NCD) with inflammation. Changes in mitochondrial function, oxidative stress and inflammation interchangeably undermine disease progression of NCD. It is not clear whether inflammation and oxidative stress are at the origin or constitute consequences of cellular pathology of NCD. Nevertheless, they significantly contribute to the pathogenesis of NCD¹ Inflammation is the host's immune response towards harmful stimuli (e.g. pathogens, dead cells, irritants) or injury. The innate immune system, that includes macrophages, has evolved to recognise and respond to pathogen-associated molecular patterns (PAMPs) including endotoxins and danger-associated molecular patterns (DAMPs) such as ATP.² As part of the host-defence mechanism, macrophages generate nitric oxide (NO) which readily reacts with superoxide (O₂⁻) to produce ONOO⁻ which contributes to tumour cell apoptosis.³ Indeed, ONOO⁻ is considered a powerful oxidant in a range of NCDs including arthritis, neurodegenerative diseases and systemic lupus erythematosus.⁴⁻⁵ The role of ONOO⁻ in NCD is largely evaluated on the presence of biomarkers such as 3-nitrotyrosine as opposed to direct measurements of ONOO⁻. Due to the complexity of ROS biology and chemistry, it is essential to develop new selective fluorescence based probes⁶ to validate signalling pathways leading to ONOO⁻ formation and use as new therapeutic probes to measure ONOO⁻ as a biomarker of disease. The main challenges of current probes include specificity issues and lack of subcellular localization. Many of the current evaluation

methods used for molecular fluorescence based sensors use exogenous ROS addition to a variety of cell lines and hence this does not allow for a true representation and understanding of the underlying biological processes. In 2005, Chang and co-workers identified peroxyresorufin-1 (PR1) as a fluorescence based sensor for H₂O₂.⁷ Cell based studies were limited to characterizing the response of PR1-loaded HEK293 cell line to the addition of exogenous H₂O₂.⁷ As boronic esters are excellent sensing groups for ONOO⁻, we hypothesize that the Chang probe PR1 is a potential tool to detect endogenous ONOO⁻ in innate immune cells. We herein report PR1 as a new red fluorescence-based tool to detect endogenous cellular ONOO⁻ formation with an improved synthesis method of PR1, and the demonstration that PR1 has higher selectivity and sensitivity towards ONOO⁻ than H₂O₂.

EXPERIMENTAL SECTION

Materials and Reagents. Unless stated otherwise, reagents and solvents were sourced from commercial suppliers, specifically: Biotium, Cayman Chemicals, Fisher Scientific, and Sigma Aldrich and were used directly as received. J774.2 macrophages (ECACC 85011428) were purchased from the European Collection of Authenticated Cell Cultures.

Synthesis of 3,7-dibromo-10H-phenoxazine. Phenoxazine (2 g, 7.38 mmol) was dissolved in chloroform (150 mL). NBS (2.63 g, 14.76 mmol) was slowly added to the mixture, which was left to stir at RT for 2 h. The mixture was quenched with

water. After separation of phases, the organic layer was washed with water (3 × 100 mL) and brine (1 × 100 mL), dried over MgSO₄, filtered and evaporated *in vacuo*. FC (SiO₂; petroleum ether/EtOAc 80:20) gave 3,7-dibromo-10*H*-phenoxazine (2 g, 80 %) as a blue solid. ¹H NMR (500 MHz, DMSO-*d*₆): δ = 6.96 – 6.85 (m, 2 H, *ArH*), 6.71 – 6.63 (m, 3 H, *ArH*), 6.06 – 5.91 (m, 2 H, *ArH*); m.p. 125 – 128 °C; IR (ATR): ν = 3393 cm⁻¹ (*w*, N–H); HR-ESI-MS: m/z (%): 363.1144 ([*M* + Na]⁺, calcd for C₁₂H₇⁷⁹Br⁸¹BrNONa⁺: 363.1104).

Synthesis of PR1. 3,7-dibromo-10*H*-phenoxazine (2.7 g, 7.92 mmol), bis(pinacolato)diboron (6.04 g, 23.76 mmol) and KOAc (4.66g, 47.52 mmol) were dissolved in DMF (100 mL), degased under argon and treated with [PdCl₂(dppf)] (579 mg, 0.792 mmol). The mixture was refluxed at 90 °C for 3 h, and cooled to RT after completion. After separation of the phases, the aqueous layer was washed with EtOAc (3 × 60 mL). The combined organic layers were washed with water (3 × 60 mL), dried over MgSO₄, filtered and evaporated *in vacuo*. FC (SiO₂; petroleum ether/EtOAc 80:20) gave 3,7-bis(4,4,5,5-tetramethyl-1,3,2-dioxaborolan-2-yl)-10*H*-phenoxazine PR1 (2.42 g, 70 %) as a dark red solid. ¹H NMR (500 MHz, DMSO-*d*₆): δ = 8.70 (s, 1 H, N-*H*), 7.04 (dd, *J* = 7.7 Hz, 1.3 Hz, 2 H, *ArH*), 6.75 (d, *J* = 7.7 Hz, 2 H, *ArH*), 6.43 (d, *J* = 1.3 Hz, 2 H, *ArH*), 1.25 (s, 24 H); m.p. 214–217 °C; IR (ATR): ν = 3404 cm⁻¹ (*w*, N–H); FTMS + *p* APCI corona MS: m/z (%): 436.2462 ([*M* + *H*]⁺, calcd for C₂₄H₃₂B₂NO₅⁺: 436.2462).

Fluorescence measurements. Fluorescence measurements were performed on a BMG Labtech CLARIOstar® using Greiner bio-one microplates, 96 well, PS, f-bottom (chimney well), black walled. Data were collected via the BMG Labtech Clariostar data analysis software package MARS. All solvents used in fluorescence measurements were HPLC or fluorescence grade and the water was de-ionised. All pH measurements taken during fluorescence/absorption experiments were recorded on a Hanna Instruments HI 9321 Microprocessor pH meter which was routinely calibrated using Fisher Chemicals standard buffer solutions (pH 4.0 - phthalate, 7.0 – phosphate, and 10.0 - borate). UV-Vis measurements were performed on a Perkin-Elmer Lambda20 Spectrophotometer, utilising Starna Silica (quartz) cuvette with 10 mm path lengths, two faces polished. Data was collected *via* the Perkin-Elmer UVWinlab software package. Phosphate buffered saline (PBS) was freshly prepared from 52 % methanol in water with KCl (10 mM), KH₂PO₄ (2.752 mM) and Na₂HPO₄ (2.757 mM). The PBS buffer was adjusted to pH 8.2 with 1 M HCl (aq). ONOO⁻ stock solutions were freshly prepared each time prior to usage. A solution of 3 M NaOH was cooled to 0 °C to which simultaneously 0.7 M H₂O₂, 0.6 M NaNO₂ and 0.6 M HCl were added. The ONOO⁻ solution was analyzed spectrophotometrically whereby the concentration of ONOO⁻ was estimated through ϵ = 1670 ± 50 cm⁻¹ M⁻¹ at 302 nm in 0.1 M NaOH (aq.). Hydrogen peroxide (H₂O₂) is commercially available whereby the concentration of H₂O₂ was determined through spectrophotometrical analysis with ϵ = 43.6 cm⁻¹ M⁻¹ at 240 nm. Sodium hypochlorite (NaOCl) is commercially available whereby the concentration of OCl⁻ was determined through spectrophotometrical analysis with ϵ = 250 cm⁻¹ M⁻¹ at 292 nm. ¹O₂ was generated by the reaction of H₂O₂ (1 mM) with NaClO (1 mM). H₂O₂ was slowly added to aq. NaOCl and stirred for 2 min. ROO• was generated from 2, 2'-azobis (2-amidinopropane) dihydrochloride. AAPH (2,2'-azobis (2-amidinopropane) dihydrochloride, 10 M) was added in de-ionized water, and then stirred at 37 °C for 30 min. O₂⁻ was

generated from KO₂ (1 eq) and 18-crown-6 (2.5 eq) dissolved in DMSO. HO• was generated by Fenton reaction: ferrous chloride (1 M) was added in the presence of 10 eq of H₂O₂ (37.0 wt%). Fluorescence titrations of ROS/RNS were carried out at 25 °C in PBS buffer pH 8.2. Different concentrations of ROS/RNS were prepared accordingly and investigated with the sensor at a concentration of 500 nM.

Cell culture. Cells are stored at -196 °C under liquid nitrogen until required. Cells are warmed up in a water bath (37 °C) for 2 min. The cell liquid was transferred into a falcon tube, to which media (5 mL) was added. The cell suspension centrifuged at 300 RCF for 5 minutes at 22 °C. After removal of the supernatant, fresh media (1 mL) was added and the cells were re-suspended and incubated at 37 °C with 5 % CO₂. J774.2 murine macrophages were grown in culture media consisting of Dulbecco's Modified Eagle's Medium/F12 (DMEM/F12) + GlutaMAX (Thermo Fisher Scientific, 31331-028) supplemented with heat inactivated Fetal Bovine Serum (FBS) (10 % v/v) (Thermo Fisher Scientific), and penicillin/streptomycin (1 % v/v) (Thermo Fisher Scientific). During cell passaging (every two days), media was removed, new media added and cells were detached with a cell scrapper and transferred to a new flask according to the protocol provided by the European Collection of Authenticated Cell Cultures.

Confocal microscopy. J774.2 macrophages were plated in an 8-well chambered cover-glass with #1.5 high performance cover glass (Cellvis, USA) at a cell density of 5 × 10⁴ cells per well in culture media (300 μL per well) and incubated at 37 °C for 16 h, in 5% CO₂. Subsequent incubation of *E. Coli* 055: B5 LPS (1 μg/ml, (Sigma Aldrich) and recombinant murine *E. Coli* IFN-γ (50 ng/ml) (PeproTech, USA) for 4 h at 37 °C. The culture media was removed, cells were washed three times with PBS (PBS was freshly prepared from milli-q water with NaCl (0.14 M), KCl (2.68 mM), Na₂HPO₄ (10.14 mM), KH₂PO₄ (1.76 mM), CaCl₂·2H₂O (0.90 mM) and MgCl₂·6H₂O (0.49 mM)). The PBS buffer was adjusted to pH 7.4 with aq. HCl), the PR1 dye (final concentration: 15 μM) and MitoView Green (final concentration: 200 nM) (Biotium, USA) in a probenecid (1 mM) (Sigma Aldrich) and Opti-MEM (Thermo Fisher Scientific) were added where indicated to the cells. The J774.2 macrophages were incubated with PR1 for 30 min at 37 °C, 5 % CO₂. The Opti-MEM-dye media was removed, cells were washed three times with PBS and replaced with a recording solution containing probenecid (1mM) in PBS for confocal microscopy. Where specified, the ONOO⁻ donor SIN-1 (Cayman Chemical, final concentration: 15 μM) was also injected after 10 min of recording. Fluorescence microscopy images were captured on a Zeiss LSM880 using 8 well chambered cover glass with #1.5 high performance cover glass (Cellvis, USA). Images were captured at different magnifications with the following parameters: MitoView Green λ_{ex} = 490 nm, λ_{em} = 523 nm and PR1 λ_{ex} = 572 nm, λ_{em} = 583 nm. Processing and analysis of confocal microscopy images were performed with Image J (NIH, Version 1.52d).

Plate Reader Recordings. Cells were plated in a Greiner bio-one black 96-well plate at a cell density of 5 × 10⁴ cells per well in culture media (200 μL per well) and incubated for 24 h, followed by incubation with LPS (100 ng/ml), IFN-γ (50 ng/ml) or both combined for 4 h at 37 °C, 5 % CO₂. PR1 (final concentration: 15 μM) was added with probenecid (1mM) in Opti-MEM to the cells and incubated for 30 min at 37 °C, 5 % CO₂. PR1 containing OptiMEM was removed, cells were washed

three times with PBS and subsequently replaced with a solution of probenecid in PBS (1 mM) for fluorescence measurements. Fluorescence intensity recordings were performed for 30 min at 37 °C.

O₂^{•-} and ONOO⁻ scavenger study. Cells were plated in a black 96-well plate at a cell density of 5 × 10⁴ cells per well in culture media (200 µL per well) and incubated for 24 h, followed by LPS (100 ng/ml) or LPS (100 ng/ml) and IFN-γ (50 ng/ml) for 4 h at 37 °C, 5 % CO₂. The culture media was removed, cells were washed three times with PBS. The scavenger (ebselen, uric acid or n-acetyl-L-cysteine at the indicated concentrations (Sigma Aldrich)) was added in Opti-MEM and incubated for 1 h at 37 °C, 5 % CO₂. After 30 min of incubation with the scavenger, PR1 (final concentration: 15 µM) in Opti-MEM was added to the cells and the cells with the dye incubated for the remaining 30 min at 37 °C, 5 % CO₂. The solutions were removed, cells were washed three times with PBS and replaced with a solution of probenecid in PBS (1 mM) for fluorescence measurements. Fluorescence intensity recordings were performed for 30 min at 37 °C.

Ebselen study. Cells were plated in a black 96-well plate at a cell density of 5 × 10⁴ cells per well in culture media (200 µL per well) and incubated for 24 h, followed by LPS (100 ng/ml) for 4 h at 37 °C, 5 % CO₂. The culture media was removed, cells were washed three times with PBS. Ebselen (final concentrations: 0.1, 0.25, 0.5, 0.75, 1 mM) in Opti-MEM was incubated for 1 h at 37 °C, 5 % CO₂. After 30 min of incubation with ebselen, the dye (final concentration: 15 µM) in Opti-MEM was added to the cells and the cells with the dye incubated for the remaining 30 min at 37 °C, 5 % CO₂. The solutions were removed, cells were washed three times with PBS and subsequently dispensed in a solution of PBS for fluorescence measurements. Fluorescence intensity recordings were performed for 30 min at 37 °C.

NOS inhibitor study. Cells were plated in a black 96-well plate at a cell density of 5 × 10⁴ cells per well in culture media (200 µL per well) and incubated for 24 h, followed by LPS (100 ng/ml) or LPS with IFN-γ (50 ng/ml) and NO scavengers (N^G-methyl-L-arginine acetate, N_w-nitro-L-arginine, at the indicated concentrations, (Sigma Aldrich)) for 4 h at 37 °C, 5 % CO₂. The culture media was removed, cells were washed three times with PBS. The PR1 dye (final concentration: 15 µM) in Opti-MEM was added to the cells and the cells with the dye incubated for 30 min at 37 °C, 5 % CO₂. The solutions were removed, cells were washed three times with PBS and subsequently replaced in a solution of PBS for fluorescence measurements. Fluorescence intensity recordings were performed for 30 min at 37 °C.

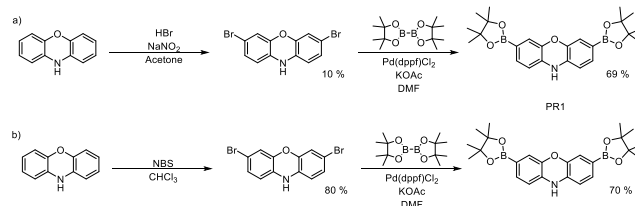
Statistical analysis. One-way analysis of variance was used for statistical analysis. The Newman-Keuls post-test was used for multiple comparisons. The results are expressed as the mean ± SEM. The differences were considered statistically significant when P values were less than 0.05. GraphPad PRISM was used for statistical analysis.

RESULTS AND DISCUSSION

Peroxyresorufin-1: synthesis and selectivity studies

The Chang synthesis of PR1 (a) involved a low yielding bromination step where HBr generated a significant number of side products.⁷ The subsequent Miyaura borylation reaction gave PR1. The overall yield of the two-step process was a low 7 %. The initial bromination step was re-evaluated and using NBS as a brominating agent resulted in an increased yield of 56 %

(Scheme 1). With an improved synthesis of PR1, fluorescence studies were performed to assess its selectivity towards different types of ROS. Chang and co-workers reported high selectivity and sensitivity towards H₂O₂ over other ROS with an enhanced fluorescence of over 1000-fold. However, boronic esters are highly effective sensing groups for ONOO⁻. Their reactivity towards ONOO⁻ is a million times faster than with H₂O₂.⁸



Scheme 1: Synthesis of PR1 – a) Procedure developed by Chang et al. 11 b) Procedure developed in this report.

In the same manner as with H₂O₂, the boronate deprotection is the underlying mechanism of PR1 with ONOO⁻. ONOO⁻ attaches to the boronate, generating an intermediate, whereby the boronate group then easily falls off generating the corresponding alcohol. In the same fashion, the other boronate group is cleaved. The alcohol group then rearranges to the ketone due to keto-enol tautomerism, affording, a well-known fluorescence based dye: resorufin. ROS selectivity studies confirmed PR1's ability to also detect ONOO⁻ with an enhanced selectivity over other ROS (Figure 1 & S4). In comparison to other ROS species, the low concentrations (50 µM vs 500 µM and 1 mM) and fast reaction time of ONOO⁻ confirm PR1's ability as a biological tool. PR1 reacts much faster with ONOO⁻ compared to H₂O₂ which is highly preferential in a biological environment where targeted detection is key. Subsequent screening of different ONOO⁻ concentrations reveals that PR1 turns on at concentrations as low as 1 µM for ONOO⁻ (Figure 2 & S-5) and saturates at 50 µM in contrast to H₂O₂ (Figure S-6 & S-7). Hence, PR1 should allow the study of biological relevant concentrations of ONOO⁻.

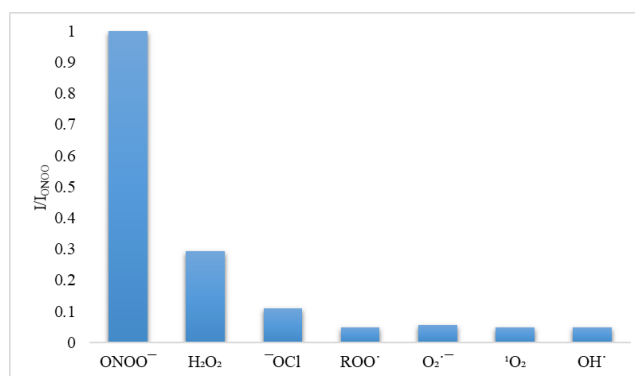


Figure 1: Selectivity data for PR1 (500 nM) in the presence of ONOO⁻ (50 µM), OH[•] (500 µM), O₂^{•-} (500 µM), ¹O₂ (500 µM) measured after 5 min. H₂O₂ (1 mM), ROO[•] (500 µM) and ·OCl (500 µM) were measured after 30 min. The data was obtained in PBS buffer 52 % H₂O:MeOH, pH = 8.2 at 25 °C at λ_{max} = 590 nm on a BMG LABTECH CLARIOstar® plate reader. Responses are blank corrected.

Validating PR1 redox sensitivity in J774.2 murine macrophages

We then set out to evaluate the generation of ONOO⁻ in J774.2 macrophages under different pro-inflammatory conditions using PR1.

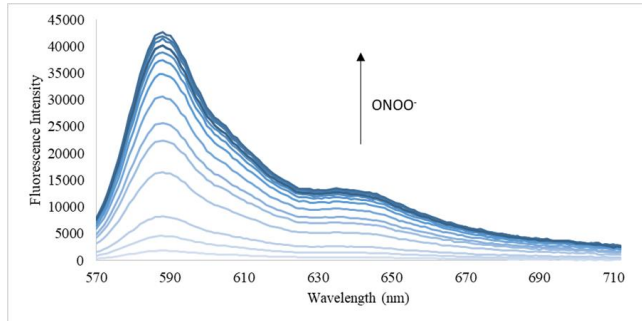


Figure 2: Emission spectra for PR1 (500 nM) in the presence of ONOO⁻ (0.5, 1, 2, 3, 4, 5, 6, 7, 8, 9, 10, 20, 50 μM) in PBS buffer 52 % H₂O: MeOH, pH = 8.2 at 25 °C. Fluorescence intensities were measured with λ_{ex} = 550 nm on a BMG Labtech CLARIOstar® plate reader. Responses are blank corrected.

Validating PR1 redox sensitivity in J774.2 murine macrophages

We then set out to evaluate the generation of ONOO⁻ in J774.2 macrophages under different pro-inflammatory conditions using PR1.

M1 Polarization and PR1 fluorescence in murine macrophages

Macrophages respond to endogenous and exogenous signals by undergoing a phenotypic change called polarization.⁹ Peripheral macrophages respond to an array of stimuli under conditions of injury and infection that lead to M1 polarization.⁹ Factors that trigger M1

polarization include bacterial LPS and the Th1 cytokine IFN-γ. A combination of LPS and IFN-γ has previously been used to enhance the production of ONOO⁻.¹⁰⁻¹¹ All recordings were performed in the presence of 1 mM probenecid to reduce the cellular efflux of PR1.¹² Using fluorescence confocal microscopy or a fluorescence plate reader, we have measured the levels of PR1 fluorescence in J774.2 macrophages primed with LPS, IFN-γ or combined priming with both factors.

First, we have evaluated the PR1 sensitivity and sub-cellular localization in murine macrophages under M1 polarizing conditions (Figure 3). In a subset of experiments, an ONOO⁻ donor (SIN-1) was added as a positive control (Figure 3, 3 a-e). We predict that PR1 will display cytosolic localization without targeting mitochondria where this was tested co-loading PR1 with a mitochondria fluorescent label, MitoView Green (Figure 3 3b, d-e). These experiments reveal an increase in PR1 fluorescence upon macrophage stimulation with LPS and IFN-γ where the fluorescence does not colocalize with MitoGreen fluorescence.

Next, we quantified PR1 fluorescence in M1 polarized macrophages using a fluorescence plate reader. Using these conditions, 50 ng/ml IFN-γ was added with 100 ng/ml LPS to enhance ONOO⁻ production (Figure 4). A combination of IFN-γ and LPS triggered a robust increase in PR1 fluorescence in macrophages compared to untreated macrophages (p ≤ 0.001, n=3) (Figure 4). Lower responses were observed with LPS or IFN-γ alone compared to combined treatment with both polarizing factors. Notably, a basal response was observed in the absence of polarizing factors that may reflect a low level of endogenous ROS production converting PR1 into fluorescent resorufin during the loading period.

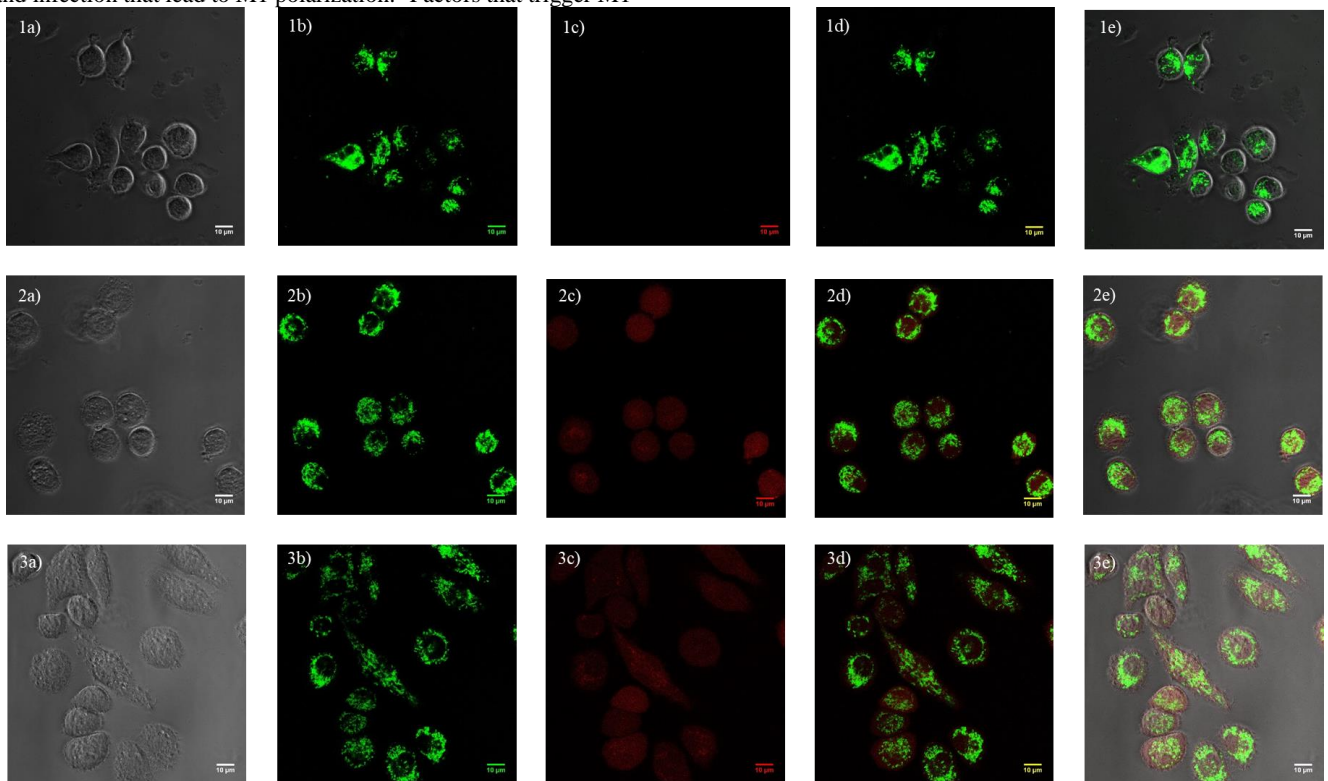


Figure 3: Confocal microscopy images of J774.2 macrophages incubated in probenecid (1mM): 1a – e: MitoView Green (200 nM); 2a – e: MitoView Green (200 nM), PR1 (15 μM) LPS (1 μg/ml) and IFN-γ (50 ng/ml); 3a – e: MitoView Green (200 nM), PR1 (15 μM), LPS (1 μg/ml), IFN-γ (50 ng/ml) and SIN-1 (15 μM). Channel (a) – Brightfield, channel (b) - λ_{ex}= 490 nm, λ_{em} = 523 nm, channel (c) - λ_{ex}= 572

nm, $\lambda_{em} = 583$ nm, channel (d) – channel (b) and (c) combined, channel (e) – channel (a), (b) and (c) combined. Magnification: $\times 63$. Scale bar: 10 μ M. $n=3$.

Evaluation of PR1 detection of endogenous ONOO⁻ production in polarized M1 macrophages

Next, we addressed whether detected PR1 fluorescence responses were due to an increase in ONOO⁻ in the macrophages. A variety of enzymatic sources generate superoxide anions (O₂⁻) that react with NO to generate ONOO⁻. Hence by inhibiting the production of either O₂⁻ or NO should lead to a decrease in ONOO⁻ production. First, we tested two O₂⁻ scavengers, ebselen¹³ and *N*-acetyl-*L*-cysteine¹⁴ (NAC). These were compared to the action of a ONOO⁻ scavenger uric acid. These were compared to the action of a ONOO⁻ scavenger uric acid. Scavengers were initially tested on LPS primed J774.2 macrophages where cells were exposed for 4 h to LPS, followed by incubation with the different scavengers (1 mM) for 1 h and incubation of PR1 (15 μ M) for 30 min (Figure 5). Uric acid, ebselen and NAC decreased PR1 fluorescence compared to untreated LPS primed macrophages ($p < 0.01$, $n=3$). Next, we further investigated the concentration dependence of the scavenger response by measuring response to different concentrations of ebselen (0.1 – 1 mM) (Figure 6).

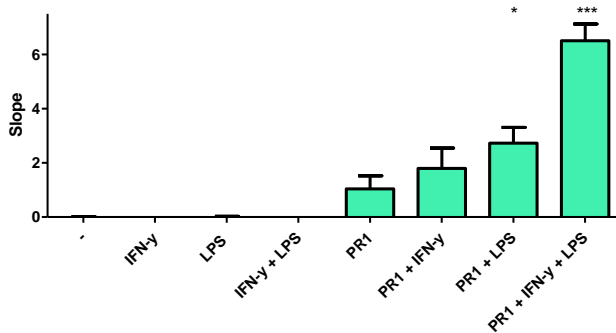


Figure 4: Rate of PR1 fluorescence in M1 polarized J774.2 macrophages. The rate of increase in PR-1 fluorescence intensity compared for unstimulated versus 100 ng/ml LPS, 50 ng/ml IFN- γ or both combined. Recordings were performed in the presence of 1 mM probenecid. Data show mean ($n=3$) \pm SEM, *** $p \leq 0.001$, * $p \leq 0.05$ with respect to PR1.

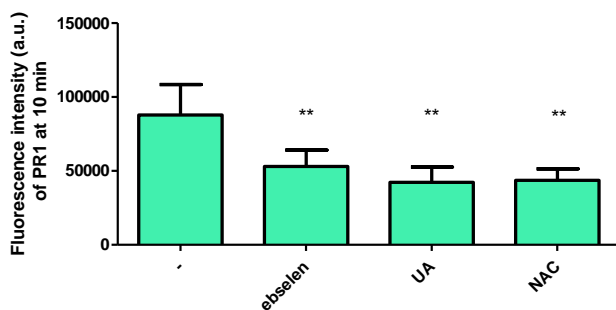


Figure 5: Effectiveness of scavengers in J774.2 macrophages. Different scavengers (ebselen, uric acid, and *N*-acetyl cysteine, final concentration: 1 mM) were investigated. Recordings were performed in the presence of 1 mM probenecid. The histogram shows the fluorescence intensity of PR1 at the time point of 10 min of recording. The ability of PR1 to detect ONOO⁻ diminishes in the usage of each scavenger with uric acid showing the most significant decrease. Data show mean values ($n=3$) \pm SEM, ** $p \leq 0.01$ with respect to control conditions.

In LPS primed macrophages, 0.25 mM ebselen decreased PR1 fluorescence where ≥ 0.5 mM ebselen gave a significant decrease compared to control LPS primed macrophages without ebselen ($p < 0.001$, $n=3$). Of note, background PR1 fluorescence in untreated macrophages was also partially reduced by 0.5 mM ebselen indicating detection of basal ROS formation. In the presence or absence of LPS, 0.5 mM ebselen reduces PR1 fluorescence to a comparable baseline level.

Having shown that we can impact O₂⁻ production in J774.2 macrophages and hence, limit ONOO⁻ formation, we then evaluated NO production. As NO is the other key component for ONOO⁻ formation, inhibiting nitric oxide synthase, a family of enzymes (NOS 1-3) that produces NO from *L*-arginine, should limit ONOO⁻ formation. In order to reduce NO production, we used 0.1 – 2 mM N^G-methyl-*L*-arginine-acetate¹⁵⁻¹⁷ and N_w-nitro-*L*-arginine.¹⁵⁻¹⁷ Both NOS inhibitors reduced PR1 fluorescence in LPS primed macrophages confirming the contribution of NO in the endogenous signal detected by PR1 as expected for the ONOO⁻ detection (Figure 7). A comparable sensitivity to both inhibitors was observed. A partial reduction of PR1 fluorescence was also observed in untreated macrophages indicating a basal ONOO⁻ formation. Overall, we conclude that PR1 detects ONOO⁻ formation in LPS primed macrophages.

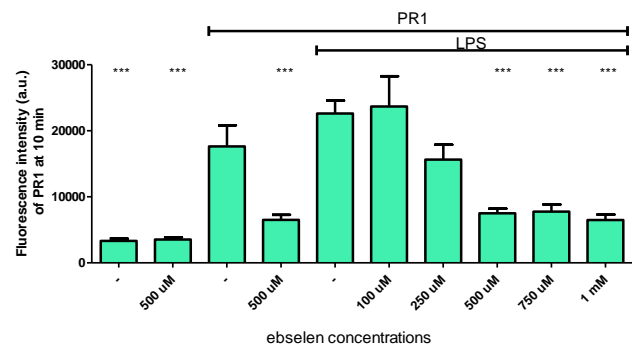


Figure 6: Effect of ebselen concentration on the scavenging of O₂⁻ consequently, limiting the ability of ONOO⁻ production. Different ebselen concentrations (0.1, 0.25, 0.5, 0.75, 1 mM) were investigated. Increasing concentrations of ebselen impact the production of O₂⁻: less O₂⁻ available, therefore less ONOO⁻ produced. Hence, the ability of PR1 to detect ONOO⁻ diminishes in fluorescence signal due to less ONOO⁻ being produced in J774.2 macrophages. Data show mean values ($n=3$) \pm SEM, *** $p \leq 0.001$ with respect to the PR1 and LPS treated group.

We next evaluated the ROS scavenger and NOS inhibitor sensitivity of PR1 fluorescence in M1 polarized macrophages (LPS and IFN- γ for 4 h). In these experiments, J774.2 macrophages were incubated with LPS (100 ng/ml), IFN- γ (50 ng/ml), NOS inhibitors (500 μ M) - N^G-methyl-*L*-arginine-acetate (NO1) and N_w-nitro-*L*-arginine (NO2) – for 4 h. After LPS, IFN- γ and NOS inhibitors treatment, uric acid (500 μ M) and ebselen (500 μ M) were incubated for 1 h. PR1 (15 μ M) was incubated for 30 min and after washing with PBS, the fluorescence intensity of PR1 was recorded. A time point of 4 min was used to evaluate the ability of PR1 to detect ONOO⁻ under the chosen conditions (Figure 8). Upon treatment of LPS and IFN- γ , high fluorescence intensity of PR1 was observed as expected when compared to control conditions. Upon introduction of NOS inhibitors, O₂⁻ and ONOO⁻ scavengers, the fluorescence signal of PR1 diminishes as expected.

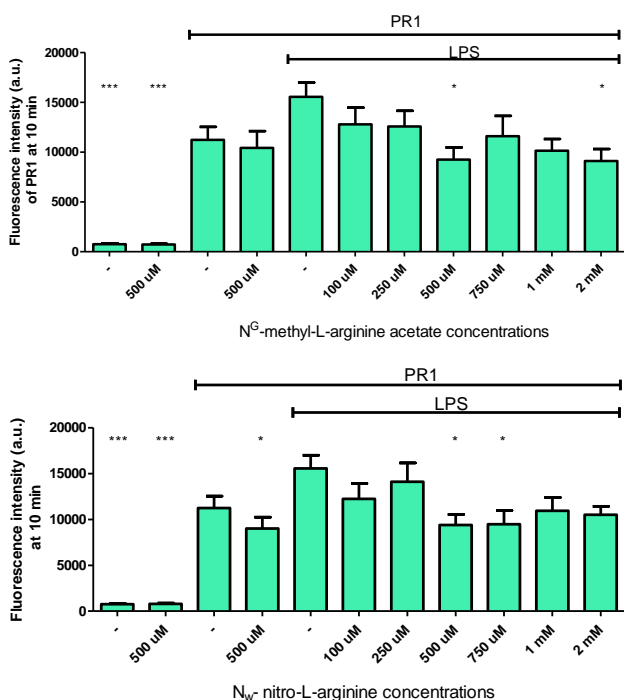


Figure 7: Effect of N^G -methyl-L-arginine-acetate and N_w -nitro-L-arginine, competitive inhibitors of NOS, on the inhibition of the catalytic production of NO from L-arginine in J774.2 macrophages. Different N^G -methyl-L-arginine-acetate and N_w -nitro-L-arginine concentrations (0.1, 0.25, 0.5, 0.75, 1, 2 mM) were investigated. Increasing concentrations of both NOS inhibitors impact towards a greater extent the catalytic production of NO. Less NO is readily available to react with O_2^- to form ONOO $^-$. Consequently, PR1 detects less ONOO $^-$ due to the diminishing fluorescence signal. Data show mean values ($n=3$) \pm SEM, *** $p \leq 0.001$, * $p \leq 0.05$ with respect to the PR1 and LPS treated group.

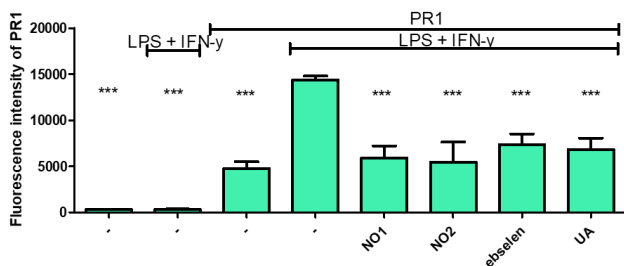


Figure 8: LPS and IFN- γ induced ONOO $^-$ production quenched by inhibitors and scavengers. The fluorescence signal of PR1 is quenched with the introduction of NOS inhibitors (N^G -methyl-L-arginine-acetate (NO1) and N_w -nitro-L-arginine (NO2)) and scavengers (ebselen and uric acid (UA)), which impact O_2^- and NO production. Data show mean values ($n=3$) \pm SEM, *** $p \leq 0.001$ with respect to PR1, LPS and IFN- γ treated group.

CONCLUSIONS

A detailed investigation of a selective and sensitive peroxynitrite sensor in J774.2 macrophages has been undertaken. We have established an improved synthetic route to PR1,⁷ and demonstrated that PR1 has greater selectivity for ONOO $^-$ compared to H_2O_2 . ROS selectivity studies confirmed high selectivity and sensitivity to ONOO $^-$ compared to a variety of other biologically important ROS. Importantly, we have shown that PR1 detects endogenous ONOO $^-$ using a combination of scavengers and NOS inhibitors in LPS-

primed and M1 polarized macrophages. Moreover, live imaging of PR1 fluorescence confirmed the cellular localisation of PR1 in polarized J774.2 macrophages. In summary we have identified PR1 as a new fluorescence tool to detect endogenous ONOO $^-$ generation that can be used for future studies to understand signalling pathways and the development of new diagnostic tools. Further work will focus on enhancing targeted organelle ROS detection in J774.2 macrophages.

REFERENCES

- Camps, J., *Oxidative stress and inflammation in non-communicable diseases-molecular mechanisms and perspectives in therapeutics*. Springer: 2014.
- Latz, E.; Xiao, T. S.; Stutz, A., Activation and regulation of the inflammasomes. *Nat. Rev. Immunol.* **2013**, *13* (6), 397-411.
- Liou, G.-Y.; Storz, P., Reactive oxygen species in cancer. *Free Radic. Res.* **2010**, *44* (5), 479-496.
- Misko, T. P.; Radabaugh, M. R.; Highkin, M.; Abrams, M.; Friese, O.; Gallavan, R.; Bramson, C.; Hellio Le Graverand, M. P.; Lohmander, L. S.; Roman, D., Characterization of nitrotyrosine as a biomarker for arthritis and joint injury. *Osteoarthr. Cartil.* **2013**, *21* (1), 151-156.
- Khan, M. A.; Alam, K.; Zafaryab, M.; Rizvi, M. M. A., Peroxynitrite-modified histone as a pathophysiological biomarker in autoimmune diseases. *Biochimie* **2017**, *140*, 1-9.
- Wang, S.; Chen, L.; Jangili, P.; Sharma, A.; Li, W.; Hou, J.-T.; Qin, C.; Yoon, J.; Kim, J. S., Design and applications of fluorescent detectors for peroxynitrite. *Coord. Chem. Rev.* **2018**, *374*, 36-54.
- Miller, E. W.; Albers, A. E.; Pralle, A.; Isacoff, E. Y.; Chang, C. J., Boronate-Based Fluorescent Probes for Imaging Cellular Hydrogen Peroxide. *J. Am. Chem. Soc.* **2005**, *127* (47), 16652-16659.
- Chen, Z.-j.; Ren, W.; Wright, Q. E.; Ai, H.-w., Genetically Encoded Fluorescent Probe for the Selective Detection of Peroxynitrite. *J. Am. Chem. Soc.* **2013**, *135* (40), 14940-14943.
- Brüne, B.; Dehne, N.; Grossmann, N.; Jung, M.; Namgaladze, D.; Schmid, T.; von Knethen, A.; Weigert, A., Redox Control of Inflammation in Macrophages. *Antioxid. Redox Signal.* **2013**, *19* (6), 595-637.
- Hou, J.-T.; Yang, J.; Li, K.; Liao, Y.-X.; Yu, K.-K.; Xie, Y.-M.; Yu, X.-Q., A highly selective water-soluble optical probe for endogenous peroxynitrite. *ChemComm* **2014**, *50* (69), 9947-9950.
- Zhang, H.; Liu, J.; Sun, Y.-Q.; Huo, Y.; Li, Y.; Liu, W.; Wu, X.; Zhu, N.; Shi, Y.; Guo, W., A mitochondria-targetable fluorescent probe for peroxynitrite: fast response and high selectivity. *ChemComm* **2015**, *51* (13), 2721-2724.
- Di Virgilio, F.; Steinberg, T. H.; Silverstein, S. C., Inhibition of Fura-2 sequestration and secretion with organic anion transport blockers. *Cell Calcium* **1990**, *11* (2), 57-62.
- Smith, Susan M. E.; Min, J.; Ganesh, T.; Diebold, B.; Kawahara, T.; Zhu, Y.; McCoy, J.; Sun, A.; Snyder, James P.; Fu, H.; Du, Y.; Lewis, I.; Lambeth, J. D., Ebselen and Congeners Inhibit NADPH Oxidase 2-Dependent Superoxide Generation by Interrupting the Binding of Regulatory Subunits. *Chem. Biol.* **2012**, *19* (6), 752-763.
- Halasi, M.; Wang, M.; Chavan, T. S.; Gaponenko, V.; Hay, N.; Gartel, A. L., ROS inhibitor N-acetyl-l-cysteine antagonizes the activity of proteasome inhibitors. *Biochemistry* **2013**, *454* (2), 201-208.
- Rotzinger, S.; Aragon, C. M. G.; Rogan, F.; Amir, S.; Amit, Z., The nitric oxide synthase inhibitor NW-Nitro-L-Arginine methylester attenuates brain catalase activity in vitro. *Life Sci.* **1995**, *56* (16), 1321-1324.
- Pfeiffer, S.; Leopold, E.; Schmidt, K.; Brunner, F.; Mayer, B., Inhibition of nitric oxide synthesis by NG-nitro-L-arginine methyl ester (L-NAME): requirement for bioactivation to the

- free acid, NG-nitro-L-arginine. *Br. J. Pharmacol.* **1996**, *118* (6), 1433-1440.
17. Peterson, D. A.; Peterson, D. C.; Archer, S.; Weir, E. K., The non specificity of specific nitric oxide synthase inhibitors. *Biochem. Biophys. Res. Commun.* **1992**, *187* (2), 797-801.

ASSOCIATED CONTENT

Supporting Information

The Supporting Information is available free of charge on the ACS Publications website.

AUTHOR INFORMATION

Corresponding Authors

* E-mail: A.Mackenzie@bath.ac.uk .T.D.James@bath.ac.uk

Author Contributions

ABM and TDJ conceived and designed the research. MW conducted all experiments and carried out data analyses. The manuscript was written by MW, ABM and TDJ. TDJ and ABM provided facilities, critically evaluated all the experiments and revised the manuscript. All authors read and approved the final manuscript.

Notes

The authors declare no financial competing interests.

ACKNOWLEDGMENTS

We would like to thank the EPSRC Centre for Doctoral Training in Sustainable Chemical Technologies (EP/ L016354/1). TDJ wishes to thank the Royal Society for a Wolfson Research Merit Award and Sophia University for a visiting professorship. We would also like to thank Dr Anne Gesell in the Bath Microscopy and Analysis Suite for training provided. This work was supported by a Biotechnology and Biological Sciences Research Council ALERT14 equipment grant (BB/M012409/1).

For TOC only

